Novel Second-Order Dual-Mode Dual-Band Filters Using Capacitance Loaded Square Loop Resonator

Sen Fu, Bian Wu, *Member, IEEE*, Jia Chen, Shou-jia Sun, and Chang-hong Liang, *Senior Member, IEEE*

***Abstract*—This paper presents a novel approach for designing dual-mode dual-band bandpass filters using capacitance loaded square loop resonators (CLSLR). The CLSLR features compactness and spurious response suppression because of the loaded capacitance. A dual-band response is obtained via an extremely large perturbation in a single resonator and second-order dual-mode dual-band filters are realized by a new cascading principle. Coupling coefficients between two resonators in both bands can be controlled independently and external quality factors are also controlled by a particularly-designed coplanar waveguide (CPW) feed line. Three types of filters are designed to validate the analysis. They are direct coupling dual-mode dual-band filter, source-load coupling dual-mode dual-band filter with a better band-to-band isolation and CPW-feed dual-mode dual-band filter with a wider bandwidth. Measured results show good agreement with the design specifications.**

***Index Terms*—Dual band, dual mode, microstrip filter, square loop.**

I. Introduction

THERE is a growing need for dual-band operation for RF devices. Several dual-band BPFs that have features of compactness, good passband, and out-of-band performances have been developed via dual-mode resonators such as microstrip patches and square loops with perturbation [1]–[6]. However, most of the proposed dual-mode dual-band BPFs are realized by two nested dual-mode resonators with different sizes [1]–[3] or by multilayer structures [4]–[6].

Several dual-mode resonators have been proposed. In [7], a new capacitively stepped impedance resonator is proposed, and another capacitively loaded square loop resonator is proposed in [8]. Using this kind of design, spurious response suppression and size reduction is realized. In [9] and [10], a cross-slot is added to increase the current transmission path, and the resonator is miniaturized. Conventional perturbation is used to stimulate the degenerate modes [1]–[6], [11], [12], but the two modes are within a single passband. In [4], [13], and [14], many ways for cascading two resonators are introduced and bandpass filters are proposed. However, the cascaded resonators are used to form only one passband. Conventional gap-coupled feeding structure for dual-mode resonators obtains a weak coupling or a high external quality factor (Q_e) within a limited range.

Therefore, only narrowband filters can be designed. A novel coplanar waveguide (CPW) feeding structure is introduced in [1]. The feeding structure results in a wide range of external quality factors and increases the design freedom.

First in this paper, a novel capacitance loaded square loop resonator (CLSLR) with spurious response suppression and size reduction is proposed. A large inner patch perturbation is designed to split the degenerate modes far away from each other so as to form two passbands. This conception is the first to be proposed. Two identical CLSLRs are cascaded by a method based on the principle of mirror which makes it possible to control the coupling strength between the two resonators in each passband independently. A CPW feed structure is explored to obtain a wider band filter. The external quality factors that are fit for both bands are realized via particularly-designed feed line.

This paper is organized as follows. Section II characterizes the proposed novel CLSLR. The way that two resonators are cascaded is demonstrated in Section III. In Section IV, three types of dual-mode dual-band filters are designed. They are direct coupling Filter I, source-load coupling Filter II, and CPW-feed Filter III. Finally, a conclusion is drawn in Section V.

II. Characteristics of Capacitance Loaded Square Loop Resonator

Fig. 1(a) depicts the proposed novel dual-mode resonator. Compared with conventional square loop dual-mode resonator, this CLSLR has four arrow-shaped patches that are attached to the outer corners of the square loop. They can act as four capacitors. Because of the loaded capacitance, the CLSLR has spurious response suppression [8]. In addition, the application of the arrow-shaped capacitance significantly increases the current transmission path at the outer corners of the loop resonator, which effectively reduces the resonance frequency and the size of the resonator. Besides, there is another important feature of the special designed patch that will be described in Section III.

The composite transmission line model of the CLSLR is shown in Fig. 1(b). It is composed of two branches in parallel, the upper one and the lower one. The loaded capacitance attached to each outer corner of the loop is equivalent to C_T, and the perturbation patch is equivalent to C_P. The characteristic impedance of the transmission line in each side of the square loop is Z_0, and its electronic length is $2\theta_0$. C_g is the input and output coupling capacitance. In order to maintain the symmetry of the circuit, $C_P + C_T$ is changed to $(C_P + C_T)/2 + (C_P + C_T)/2$ in the upper branch, and C_T is changed to $C_T/2 + C_T/2$ in the lower branch.

Manuscript received July 07, 2011; revised December 19, 2011; accepted December 20, 2011. Date of publication February 06, 2012; date of current version March 02, 2012. This work is supported by the National Natural Science Foundation of China (NSFC) under project 60901031 and the Fundamental Research Funds for the Central Universities 72005477.

The authors are with the National Key Laboratory of Antennas and Microwave Technology, Xidian University, Xi'an, 710071, China (e-mail: fusensam3@gmail.com).

Color versions of one or more of the figures in this paper are available online at http://ieeexplore.ieee.org.

Digital Object Identifier 10.1109/TMTT.2011.2181859

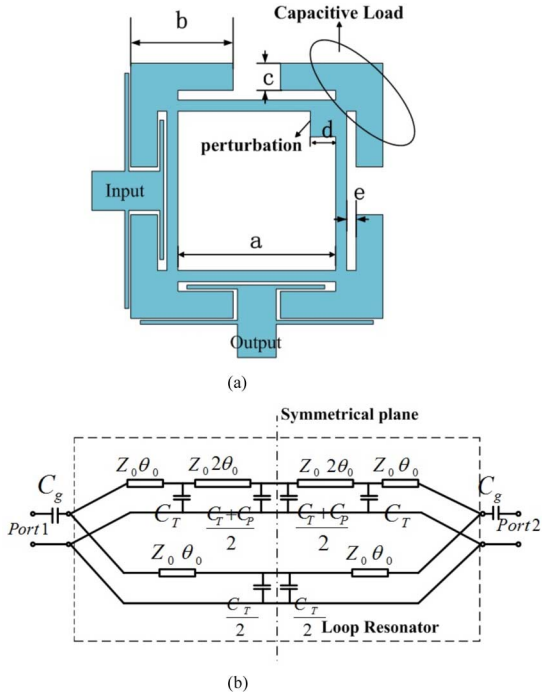

Fig. 1. (a) Configuration of the proposed capacitance loaded square loop resonator (CLSLR). (b) Composite transmission line model.

The circuit model in Fig. 1(b) can be analyzed using even–odd-mode analysis. The even-mode circuit is achieved by adding a magnetic wall along the symmetrical plane which can be seen as an open circuit. Since the equivalent circuit is in a shunt configuration, its input admittance $Y_{\text{in\_even}}$ from Port1 is derived as follows:

$$Y_{\text{in\_even}} = Y_{1\_\text{even}} + Y_{2\_\text{even}} \tag{1a}$$

where

$$Y_{1\_\text{even}} = \frac{Y'_{1\_\text{even}} Z_0 + j\tan\theta_0}{Z_0(1 + jY'_{1\_\text{even}} Z_0 \tan\theta_0)} \tag{1b}$$

$$Y'_{1\_\text{even}} = j\omega C_T + j\frac{\omega Z_0\left(\frac{C_P+C_T}{2}\right) + \tan 2\theta_0}{Z_0\left[1 - \omega Z_0\left(\frac{C_P+C_T}{2}\right)\tan 2\theta_0\right]} \tag{1c}$$

$$Y_{2\_\text{even}} = j\frac{\omega Z_0\left(\frac{C_T}{2}\right) + \tan\theta_0}{Z_0\left[1 - \omega Z_0\left(\frac{C_T}{2}\right)\tan\theta_0\right]}. \tag{1d}$$

The odd-mode circuit is achieved by adding an electric wall along the symmetrical plane which can be seen as a short circuit. Its input admittance $Y_{\text{in\_odd}}$ from Port1 is derived as (2a)–(2d):

$$Y_{\text{in\_odd}} = Y_{1\_\text{odd}} + Y_{2\_\text{odd}} \tag{2a}$$

where

$$Y_{1\_\text{odd}} = \frac{Y'_{1\_\text{odd}} Z_0 + j\tan\theta_0}{Z_0(1 + jY'_{1\_\text{odd}} Z_0 \tan\theta_0)} \tag{2b}$$

$$Y'_{1\_\text{odd}} = j\omega C_T + \frac{1}{jZ_0\tan 2\theta_0} \tag{2c}$$

$$Y_{2\_\text{odd}} = \frac{1}{jZ_0\tan\theta_0}. \tag{2d}$$

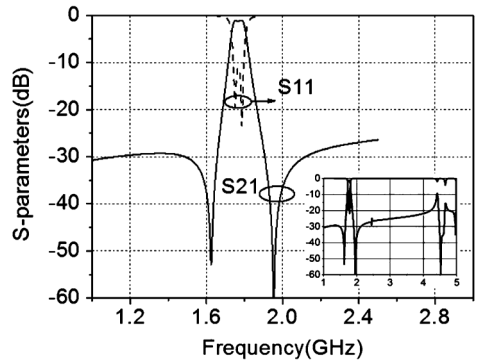

Fig. 2. Simulated S-parameters of the proposed CLSLR. Out-of-band performance is plotted in inset from 1 to 5 GHz.

The square loop will resonate when its input admittance equals to zero, which is expressed as $Y_{\text{in\_even}} = 0$ for even mode and $Y_{\text{in\_odd}} = 0$ for odd mode.

It should be mentioned that (1a)–(1d) and (2a)–(2d) show that the perturbation C_P affects the even-mode resonance frequency but has no relationship with the odd-mode one. Fig. 3(b) shows the resonance frequencies of the even mode and odd mode against perturbation size d. The reason that the odd-mode resonance frequency has a minor change is that the length of the transmission line adjacent to the perturbation patch is disturbed when the perturbation size changes.

Simulation of the CLSLR is done by the commercial simulator Zeland IE3D, and the result is presented in Fig. 2. It shows that the first and second spurious respond are suppressed under 20 dB.

It is known that two degenerate modes with a 90° phase offset are stimulated when a perturbation is added in the symmetrical plane of a loop resonator. Conventionally, the perturbation size is relatively small so that the two modes couple with each other through the perturbation to form one passband. What if the size of the perturbation increases to an extremely large value? Fig. 3(a) shows simulated S21 with different perturbation size. Fig. 3(b) shows the resonance frequencies of even mode and odd mode against the perturbation size d. The odd mode (hereinafter low mode) changes within a small range, but the even mode (hereinafter, high mode) changes rapidly. If the perturbation size is large enough to split the two modes far away from each other to form two passbands that we need, a second-order dual-mode dual-band bandpass filter will be achieved via cascading two resonators. This conception is rarely proposed before.

III. Coupling Properties of Dual-Mode Dual-Band Filter

The key point in designing dual-band filters is to meet coupling coefficients of both passbands, especially for dual-mode filters. A method for controlling coupling strength of the two pairs of modes completely and independently is proposed in this paper.

Resonance frequencies of two degenerate modes in a resonator have a 90° phase offset, which is the same as their electronic fields or current distributions. Fig. 4 shows the average

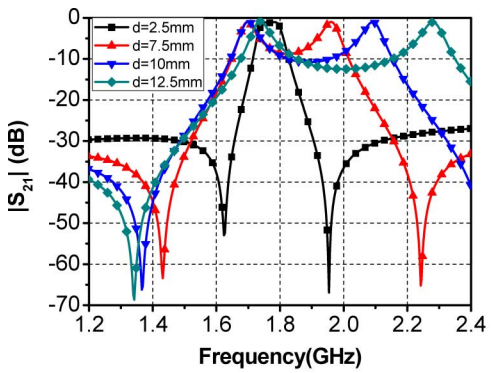

(a)

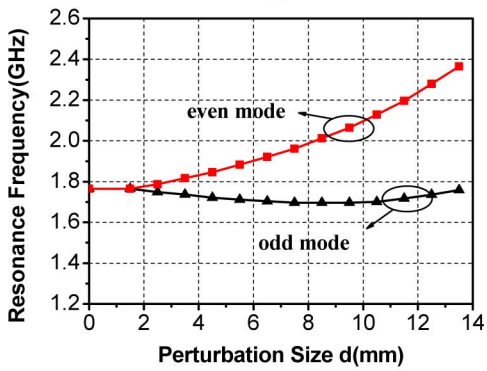

(b)

Fig. 3. (a) Simulated S-parameter with different perturbation size (d = 2.5 mm, d = 7.5 mm, d = 10 mm, and d = 12.5 mm). (b) Resonance frequencies of odd mode and even mode against perturbation size d.

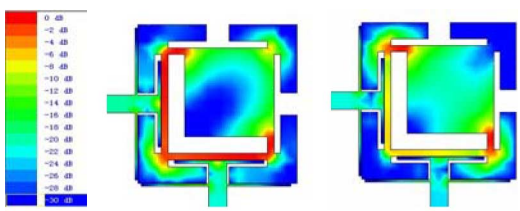

(a) (b)

Fig. 4. Average current distribution of CLSLR with a large enough perturbation size d = 12.5 mm. (a) Low-mode resonance frequency of 1.735 GHz. (b) High-mode resonance frequency of 2.28 GHz.

current distribution of CLSLR with an extremely large perturbation size. The average currents of the low mode and the high mode are distributed along the two vertical diagonals, respectively, especially at the corners. If two resonators are cascaded, the corners where the currents of the high modes/low modes are distributed should be close to each other.

Dual-mode resonators are cascaded in many ways because of the various locations of perturbation and feed line. However, there is no effective way that can control the coupling strength of low modes and high modes between two resonators, respectively. The mirror principle will be used to cascade two CLSLRs in this paper for a dual-mode dual-band filter.

A sketch map of the principle is shown in Fig. 5 to illustrate how the two resonators are cascaded. Main currents of high modes in the two resonators are distributed at corner ① and

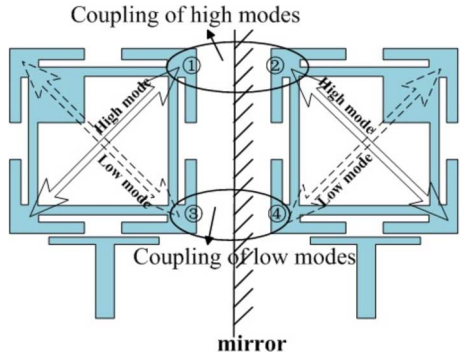

Fig. 5. Sketch map of the mirror principle. (Solid arrow shows the main electronic field of high mode. Dashed arrow shows the main electronic field of low mode.)

corner ②, respectively, and the main currents of the low modes are distributed at corner ③ and corner ④. Then, the two pairs of modes can couple through the gap between the two resonators, respectively. Because of the open space between corner ① and corner ③ or corner ② and corner ④, the two pairs of modes are able to couple effectively and do not disturb each other. This is another important feature of the special designed patches that attached to the outer corners of the square loop.

This principle will be validated by the model shown in Fig. 6(a). Fig. 6(b) shows the topology of the dual-mode dual-band filter. In order to decrease the effect of input–output on the coupling coefficients between the two resonators, a weak input–output feed is used in this filter. Because the distance between the two resonators will affects the high-mode and low-mode coupling coefficients at the same time, g must be adjusted to a suitable distance and then remains unchanged for a fixed low-mode coupling coefficient. Then, a transmission line segment (hereinafter coupled line) is added along corner ① and corner ②. It is utilized to control high-mode coupling coefficient by adjusting L.

Fig. 7 shows the simulation result when g = 0.5 mm. Fig. 7(a) visually displays the changes of coupling strength when L = 0.5, 2.5, and 5 mm, while Fig. 7(b) depicts how the low-mode and high-mode coupling coefficients vary with the length of L. The change of L will not affect the low-mode coupling coefficient, but it can affect the high-mode coefficient. It proves that there is no interaction between the low-mode coupling and high-mode coupling if the two CLSLRs are cascaded in this way. Therefore, the coupling strength of the two pairs of modes can be controlled independently.

Vice versa, adjust g to a suitable distance and keep it unchanged for a fixed high modes coupling coefficient and add a coupled line along corner ③ and corner ④ to control low-mode coupling coefficient by adjusting L. However, the difficulty is that the location of the coupled line has been taken by the external feed line, but it can be overcome by the CPW feed, which will be used in the next section.

IV. Design of Dual-Mode Dual-Band Filters

This section will show three design examples of second-order dual-mode dual-band filters based on the above method.

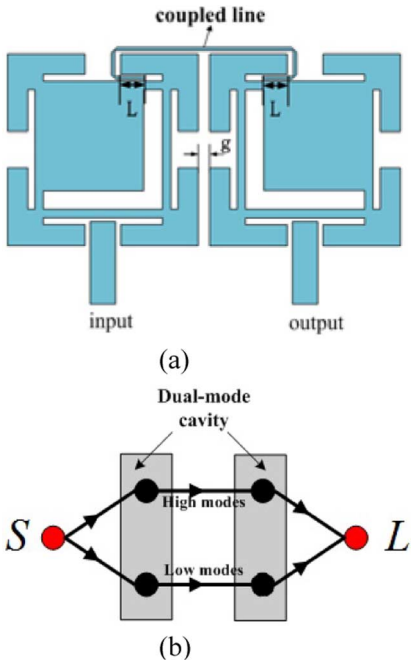

Fig. 6. (a) Configuration of two cascaded CLLDRs. (b) Topology of the dual-mode dual-band filter.

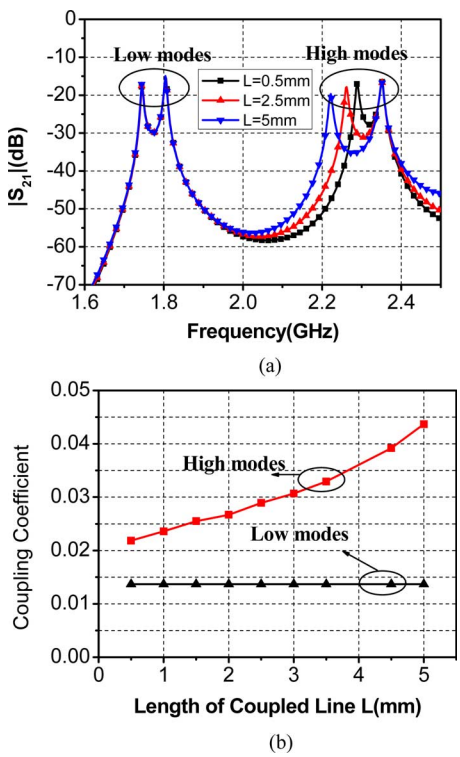

Fig. 7. (a) Simulated S21 parameter of cascaded CLSLRs with different L ($L = 0.5$, 1.5, and 5 mm). (b) Calculated coupling coefficients of high modes and low modes against L.

A. Direct Coupling Dual-Mode Dual-Band Filter I

Design specifications of the filter are shown in Table I. A lot of work has been done on filter synthesis in [15]. Coupling matrix is used in designing filters.

The [N + 2] ideal coupling matrix M of the first passband and second passband is derived as (3a). The actual coupling

TABLE I
DESIGN SPECIFICATIONS OF FILTER I

	f_0 / MHz	BW / MHz	Return Loss	FBW
Band I	1800	40	10 dB	2.22%
Band II	2360	40	10 dB	1.70%

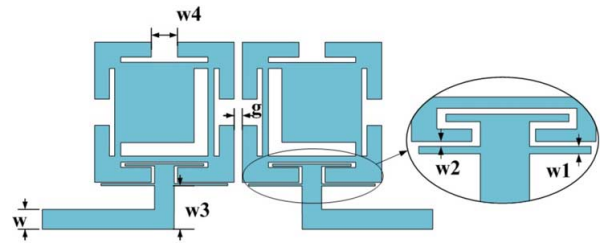

Fig. 8. Configuration of the proposed direct coupling second-order dual-mode dual-band Filter I. Dimensions of Filter I are a = 15 mm, b = 10.3 mm, c = 2.5 mm, d = 12.5 mm, e = 1 mm, g = 0.9 mm, w = 2.7 mm, w1 = 0.4 mm, w2 = 0.1 mm, w3 = 8.8 mm, w4 = 3.4 mm ($\varepsilon_r = 2.5$ $h = 1$ mm).

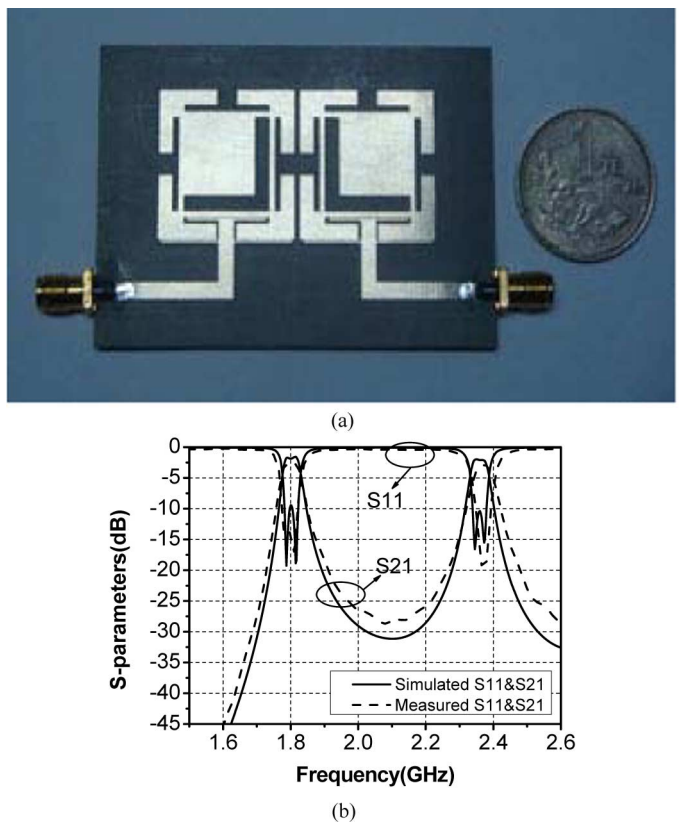

Fig. 9. (a) Photograph of the fabricated Filter I. (b) Simulated and measured results of Filter I.

coefficients and external Q_e can be computed from matrix M using equations as (3b).

$$M_1 = M_2 \begin{bmatrix} 0 & M_{S1} & 0 & 0 \\ M_{1S} & 0 & M_{12} & 0 \\ 0 & M_{21} & 0 & M_{2L} \\ 0 & 0 & M_{L2} & 0 \end{bmatrix} = \begin{bmatrix} 0 & 0.8575 & 0 & 0 \\ 0.8575 & 0 & 1.0201 & 0 \\ 0 & 1.0201 & 0 & 0.8575 \\ 0 & 0 & 0.8575 & 0 \end{bmatrix} \quad (3a)$$

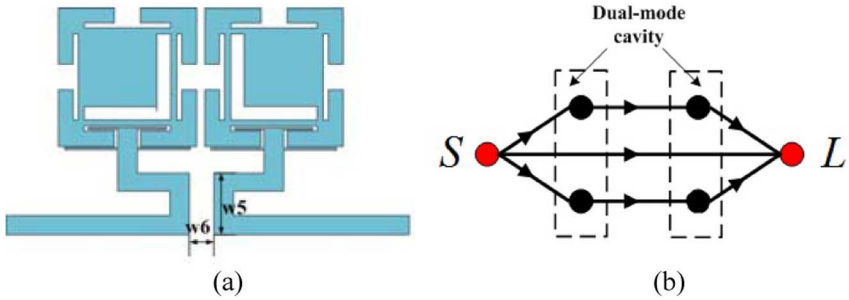

Fig. 10. (a) Configuration of Filter II. The dimensions are $w5 = 10.2$ mm, $w6 = 1.3$ mm. Other dimensions are the same as Filter I. (b) Topology of Filter II.

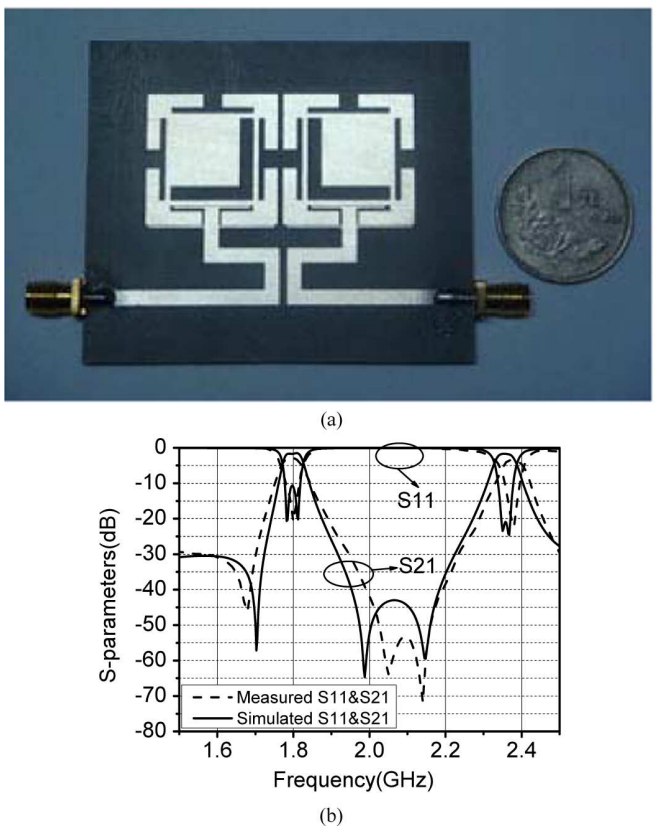

Fig. 11. (a) Photograph of the fabricated Filter II. (b) Simulated and measured results of Filter II.

$$m_{ij} = FBW \cdot M_{ij}$$
$$Q_e = \frac{1}{FBW \cdot M_{S1}^2}. \tag{3b}$$

Then, the coupling coefficients and Q_e of the two passbands are $m_{12} = m_{21} = 0.0224, Q_e = 61.30$ for passband one, and $m_{12} = m_{21} = 0.0173, Q_e = 80.20$ for passband two.

The configuration and dimensions of the proposed second-order dual-mode dual-band bandpass Filter I are shown in Fig. 8. The length of g must first be confirmed for the coupling coefficient 0.0224 of the first band and then a coupled line must be added to adjust the coupling coefficient of the second band. Coincidentally, the coupling coefficient of the second passband fits well without the coupled line. Fig. 9(a) shows the photograph of the fabricated dual-mode dual-band filter, and the simulated and measured results are illustrated in Fig. 9(b), which shows

TABLE II
DESIGN SPECIFICATIONS OF FILTER III

	f_0 / MHz	BW / MHz	Return Loss	FBW
Band I	2000	150	15 dB	7.5%
Band II	2760	150	15 dB	5.43%

that the design specification is well satisfied. The measured result of the fabricated filter has a good agreement with the simulation response. The measured band-to-band isolation is better than 25 dB at 2.1 GHz.

B. Source-Load Coupling Dual-Mode Dual-Band Filter II

Direct coupling bandpass filters have a relatively poor out-of-band rejection without transmission zeros. A source-load coupling dual-mode dual-band filter is designed for a better out-of-band rejection and band-to-band isolation.

Filter II has the same design specifications as Filter I, and its configuration and topology are shown in Fig. 10. Fig. 11(a) shows the photograph of the fabricated Filter II, and the simulated and measured results are illustrated in Fig. 11(b). Two transmission zeros are brought in between the first and second band at 1.98 and 2.15 GHz, and one is brought in at 1.7 GHz in the simulation. The measured transmission zeros are at 1.7, 2.05, and 2.15 GHz. The measured band-to-band isolation is better than 50 dB at 2.1 GHz.

C. CPW-Feed Dual-Mode Dual-Band Filter III

Filters that are fed by gap-coupling like Filter I and Filter II have a weak coupling strength or high external quality factor (Q_e) within a limited range usually no lower about 50 [1]. However, the CPW-feed can effectively decrease the value of Q_e and increase the design freedom.

Design specifications of the CPW-feed filter are shown in Table II. The ideal coupling matrix of the first passband and second passband is derived as follows:

$$M_1 = M_2 = \begin{bmatrix} 0 & 1.0371 & 0 & 0 \\ 1.0371 & 0 & 1.286 & 0 \\ 0 & 1.286 & 0 & 1.0371 \\ 0 & 0 & 1.0371 & 0 \end{bmatrix}. \tag{4}$$

The coupling coefficients and Q_e of the two passbands can be derived from (3b): $m_{12} = m_{21} = 0.0965, Q_e = 12$ for passband one, and $m_{12} = m_{21} = 0.0699, Q_e = 17$ for passband two.

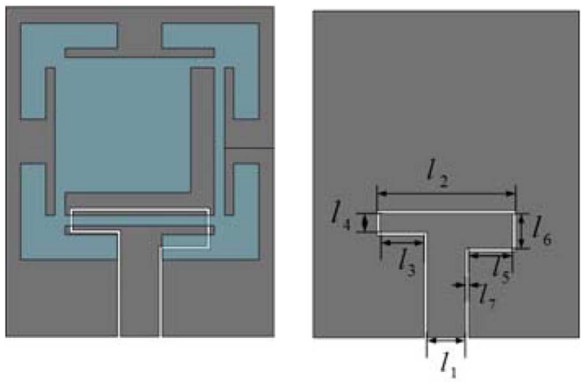

(a) (b)

Fig. 12. Configuration of the CPW-feed structure. (a) Top view (b) Bottom view. The dimensions are $l_1 = 2.4$ mm, $l_2 = 12.5$ mm, $L = 1.2$ mm, $l_5 = 4.8$ mm, $l_6 = 3$ mm, $l_7 = 0.5$ mm, $c = 1.5$ mm. Other dimensions of CLSLR are the same as Filter I.

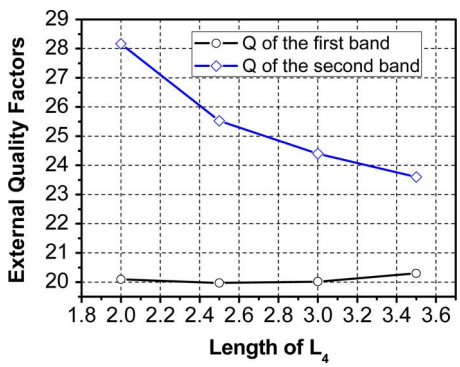

Fig. 13. Q factors of the two passbands against the length of l_4.

The external quality factors in this dual-band filter are 12 and 17. Since the gap-coupling feed cannot satisfy them, the CPW-feed structure will be used. It is important to control both the external quality factors of the two passbands. Filters in the form of nested resonators have been proposed before [2], [3], and both external quality factors can be controlled by CPW-feed.

However, no solutions have been given in the case of a single resonator. A method is proposed in this paper to control both external quality factors in the case of a single resonator.

The CPW-feed structure is shown in Fig. 12. There are two branches in the end of the feed line. It has been analyzed in Section III that the main currents of the high mode and low mode are distributed in different corners, so the area of the left branch and right branch has a different effect on the external quality factors of the two passbands. In order to show how the two branches affect the external quality factors, the area of the right branch is fixed, and the area of the left branch will be changed. To be simple, Fig. 13 just shows the external quality factors against the width of l_4, while l_3 keeps constant and equals to $l_5 = 3.5$ mm. It is obvious that the external quality factor of the second passband changes quickly with different l_4, while the external quality factor of the first passband almost keeps unchanged. If l_3 and l_4 are adjusted simultaneously, a wider range of Q will be achieved. Therefore, if the area of the two branches is proper, the needed external quality factors of the two passbands will be obtained.

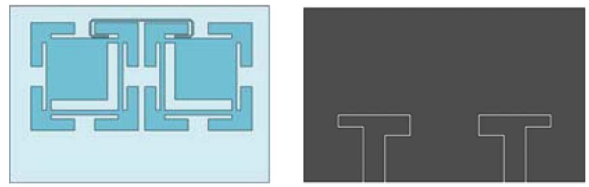

(a) (b)

Fig. 14. Configuration of the CPW-feed dual-mode dual-band Filter III. (a) Top view (b) Bottom view. The dimensions are $c = 1.5$ mm, $l_1 = 2.4$ mm, $l_2 = 12.5$ mm, $l_3 = 5.3$ mm, $l_4 = 1.5$ mm, $l_5 = 3.8$ mm, $l_6 = 3$ mm, $l_7 = 0.5$ mm, $L = 1.2$ mm. Other dimensions of CLSLR are the same as Filter I.

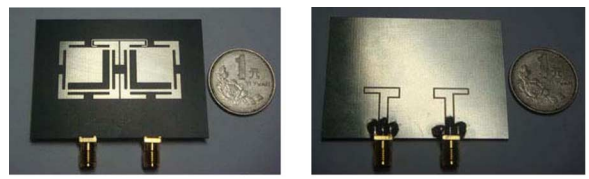

(a) (b)

Fig. 15. Photographs of the fabricated CPW-feed dual-mode dual-band Filter III. (a) Top view. (b) Bottom view.

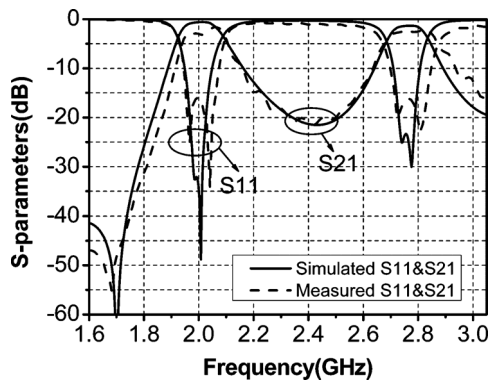

Fig. 16. Simulated and measured results of Filter III.

TABLE III
COMPARISON OF THE THREE FILTERS

	Band I		Band II		Isolation
	f_0/GHz	FBW	f_0/GHz	FBW	
Filter I	1.8	2.22%	2.36	1.70%	25 dB
Filter II	1.8	2.22%	2.36	1.70%	50 dB
Filter III	2	7.5%	2.76	5.43%	20 dB

The configuration of the CPW-feed dual-mode dual-band Filter III is shown in Fig. 14. The photographs of the fabricated filter are shown Fig. 15, and the simulated and measured results are illustrated in Fig. 16, which shows that the design specification is well satisfied. The measured result of the fabricated filter has a good agreement with the simulation response. The measured band-to-band isolation is better than 20 dB at 2.4 GHz. The comparison of the three filters is presented in Table III.

V. CONCLUSION

In this paper, a novel dual-mode resonator is proposed, and a new approach has been presented to design dual-mode dual-

band filters via cascading two resonators. The coupling coefficients and external quality factors in both bands can be controlled independently. Three dual-mode dual-band filters are design for validating the analysis. The source-load coupling filter has a better out-of-band rejection and band-to-band isolation compared with the direct coupling filter. The CPW-feed filter has a wider band and a greater design freedom. Better performances may be realized by multi-order filters. The measured results agree well with the simulation.

REFERENCES

[1] X. Y. Zhang and Q. Xue, "Novel dual-mode dual-band filters using coplanar-waveguide-fed ring resonators," *IEEE Trans. Microw. Theory Tech.*, vol. 55, no. 10, pp. 2183–2190, Oct. 2007.

[2] J.-W. Baik, L. Zhu, and Y.-S. Kim, "Dual-mode dual-band bandpass filter using balun structure for single substrate configuration," *IEEE Microw. Wireless Compon. Lett.*, vol. 20, no. 11, pp. 613–615, Nov. 2010.

[3] J.-W. Baik, S. Pyo, W.-S. Yoon, and Y.-S. Kim, "Dual-mode dual-band bandpass filter for single substrate configuration," *Electron. Lett.*, vol. 45, no. 19, Sept. 2009.

[4] E. E. Djoumessi and K. Wu, "Multilayer dual-mode dual-bandpass filter," *IEEE Microw. Wireless Compon. Lett.*, vol. 19, no. 1, pp. 21–23, Jan. 2009.

[5] J.-X. Chen, T. Y. Yum, J.-L. Li, and Q. Xue, "Dual-mode dual-band bandpass filter using stacked-loop structure," *IEEE Microw. Wireless Compon. Lett.*, vol. 16, no. 9, pp. 502–504, Sep. 2006.

[6] H. M. Hizan, I. C. Hunter, and A. I. Abunjaileh, "Integrated dual-band radiating bandpass filter using dual-mode circular cavities," *IEEE Microw. Wireless Compon. Lett.*, vol. 21, no. 5, pp. 246–248, May 2011.

[7] S.-W. Fok, P. Cheong, K.-W. Tam, and R. P. Martins, "A novel microstrip square-loop dual-mode bandpass filter with simultaneous size reduction and spurious response suppression," *IEEE Trans. Microw. Theory Tech.*, vol. 54, no. 5, pp. 2033–2041, May 2006.

[8] P. Cheong, T.-S. Lv, W.-W. Choi, and K.-W. Tam, "A compact microstrip square-loop dual-mode balun-bandpass filter with simultaneous spurious response suppression and differential performance improvement," *IEEE Microw. Wireless Compon. Lett.*, vol. 21, no. 2, pp. 77–79, Feb. 2011.

[9] L. Zhu, B. C. Tan, and S. J. Quek, "Miniaturized dual-mode bandpass filter using inductively loaded cross-slotted patch resonator," *IEEE Microw. Wireless Compon. Lett.*, vol. 15, no. 1, pp. 22–24, Jan. 2005.

[10] W.-H. Tu and K. Chang, "Miniaturized dual-mode bandpass filter with harmonic control," *IEEE Microw. Wireless Compon. Lett.*, vol. 15, no. 12, pp. 838–840, Dec. 2005.

[11] A. Görür, "Description of coupling between degenerate modes of a dual-mode microstrip loop resonator using a novel perturbation arrangement and its dual-mode bandpass filter applications," *IEEE Trans. Microw. Theory Tech.*, vol. 52, no. 2, pp. 671–677, Feb. 2004.

[12] B. T. Tan, J. J. Yu, S. T. Chew, M.-S. Leong, and B.-L. Ooi, "A miniaturized dual-mode ring bandpass filter with a new perturbation," *IEEE Trans. Microw. Theory Tech.*, vol. 53, no. 1, pp. 343–348, Jan. 2005.

[13] J. A. Curtis and S. J. Fiedziuszko, "Miniature dual mode microstrip filters," *IEEE MTT-s Dig.*, pp. 443–446, 1991.

[14] J. A. Curtis and S. J. Fiedziuszko, "Multi-layered planar filters based on aperture coupled, dual mode microstrip or stripline resonators," *IEEE MTT-s Dig.*, pp. 1203–1206, 1992.

[15] R. J. Cameron, "General coupling matrix synthesis methods for Chebyshev filtering functions," *IEEE Trans. Microw. Theory Tech.*, vol. 47, no. 4, pp. 433–442, Apr. 1999.

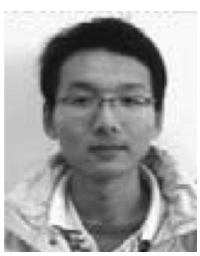

Sen Fu was born in Shijiazhuang, Hebei Province, China, in 1986. He received the B.S. degree in electronic and information engineering from Xidian University, Xi'an, China, in 2009. He is currently working towards the M.S. degree in electromagnetic and microwave technology at Xidian University.

His research interests are RF/microwave passive structures, include microwave filters, metamaterials, and millimeter-wave circuits and components.

Bian Wu (S'08–M'09) was born in Xianning city, Hubei Province, China, in 1981. He received the B.Eng. degree in electronic and information engineering and the Ph.D. degree in electromagnetic and microwave technology from Xidian University, Xi'an, China, in 2004 and 2008, respectively.

Since 2008, he has been a Lecturer at Xidian University, and is currently an Associate Professor with the Science and Technology on Antenna and Microwave Laboratory at Xidian University. His research interests include microwave filters and multiplexers, planar miniaturized antennas, EBG, and left-handed materials and computational electromagnetic.

Dr. Wu is a member of the IEEE Microwave Theory and Techniques (MTT) Society and a member of the Chinese Institute of Electronics.

Jia Chen was born in Henan, China. He received the B.S. and M.S. degrees from the School of Electronic Engineering from Xidian University, Xi'an, China, in 2007 and 2010, respectively. He is currently working towards the Ph.D. degree in electromagnetic fields and microwave technology.

His research interests include the design of microwave filters and associated RF modules for Microwave and advanced microwave and millimeter-wave circuits and components.

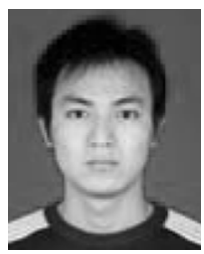

Shou-jia Sun was born in Anhui Province, China. He received the B.S. degree from the School of Electronic Engineering from Xidian University, Xi'an, China, in 2009. He is currently working towards the Ph.D. degree in electromagnetic fields and microwave technology.

His research interests include the design of microwave filters and planar antennas and EBG and multiplexers and computational electromagnetic.

Chang-hong Liang (M'80–SM'83) was born in Shanghai, China, on December 9, 1943. He graduated in 1965 from the former Xidian University, Xi'an, China, and continued his graduate studies until 1967.

From 1980 to 1982, he was a visiting scholar at Syracuse University, Syracuse, NY. He has been a Professor and Ph.D. student advisor at Xidian University since 1986. He has wide research interests, which include computational microwave and computational electromagnetics, microwave network theory, microwave measurement method and data processing, lossy variational electromagnetics, electromagnetic inverse scattering, and electromagnetic compatibility.

Prof. Liang was awarded a number of titles, including the National Middle-Aged and Young Expert with Distinguished Contribution, the National Excellent Teacher, and One of the 100 National Prominent Professors. He is a Fellow of the CIE.